Turbulent Hot Jet Ignition of Ultra-Lean H_2/Air Mixtures: Influence of the Orifice Diameter

J. Höltkemeier-Horstmann, D. Markus, S. Essmann
Physikalisch-Technische Bundesanstalt
Braunschweig, Lower Saxony, Germany

1 Introduction

Hydrogen is an attractive energy carrier for future applications such as heavy-duty engines or long-range trucking [1], its main benefit over conventional fuels being that carbon dioxide emissions from combustion cannot occur. One drawback of using hydrogen as a fuel is a high adiabatic flame temperature which leads to significant thermal NO_x emissions [2, 3]. An approach to lower NO_x emissions is to reduce the flame temperature by exhaust gas recirculation [2, 4] where the oxygen concentration is reduced. However, at high air-fuel equivalence ratio ($\lambda > 3$), more energy is required to ignite the mixture and the laminar flame speed of hydrogen decreases, leading to lower combustion efficiency [4–6]. Turbulent hot jet ignition (THJI) is a concept addressing both issues in which a near-stoichiometric mixture is ignited by a spark plug in a pre-chamber [5, 7–9]. A hot exhaust gas jet enters the main combustion chamber via a number of nozzles, leading to ignition across a large volume and to a faster burn rate.

In this work, THJI of lean and ultra-lean hydrogen air mixtures is studied in a two-chamber model setup. Pressure and schlieren measurements are employed to investigate the ignition process. The effects of THJI as opposed to ignition by a spark plug are explored for three nozzle diameters. The parameters analysed are the maximum explosion pressure, the rate of pressure rise and the delay time between spark ignition and maximum pressure. The results can be used to optimize THJI systems for lean hydrogen ignition.

2 Experimental Setup

The test vessel had a main chamber volume of 13 L and a pre-chamber to main chamber volume ratio of 0.1 %. Three different pre-chamber orifice diameters were tested (1.0 mm, 1.2 mm and 1.4 mm). A spark plug (Kistler 6113) was used to ignite the stoichiometric mixture inside the pre-chamber. A schematic drawing of the vessel including gas supply and gas analysis is shown in Fig. 1. Two mass flow controllers (Bronkhorst EL-Flow) each were used for main chamber and pre-chamber hydrogen/air mixture preparation. An oxygen analyser (Servomex OxyExact2223) was used to control the mixture composition in each chamber separately. For each orifice diameter a bisection method was used to find the ignitability limit until the resolution limit of 2 % in λ.

Correspondence to: jacqueline.horstmann@ptb.de

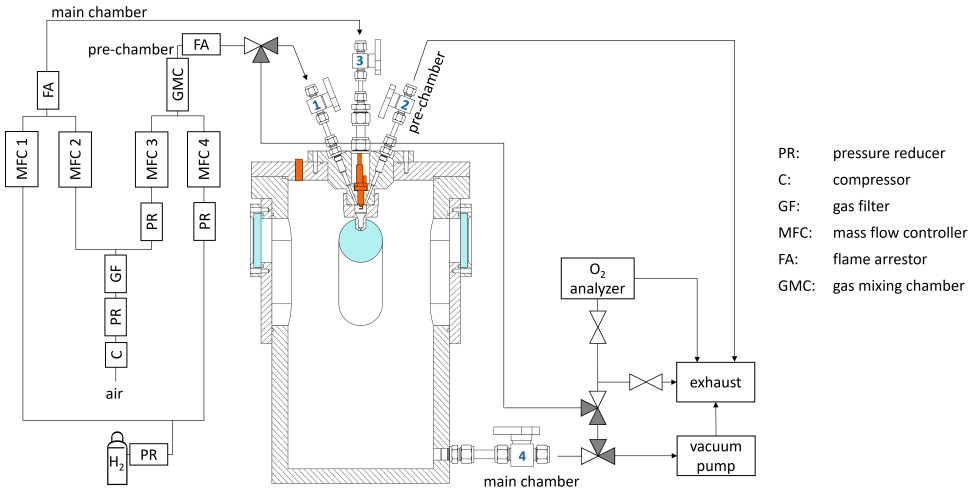

Figure 1: Test chamber with gas supply. Piezo-electric pressure sensor and spark plug with integrated piezo-electric pressure sensor marked in orange.

2.1 Mixture preparation

The correct mass flow controller settings for pre-chamber gas supply were determined by oxygen analysis. The necessary gas flow to ensure that there was no gas-flow from the main chamber to the pre-chamber and only a small gas flow from the pre-chamber to the main chamber during flushing was determined by schlieren measurements before and observed while flushing. First, the main-chamber gas supply was started and the evolution of the oxygen concentration was controlled after passing the chamber. At constant mixture composition, the pre-chamber gas supply was started additionally and run for 10 minutes. The valves were closed in the following sequence (according to the labelling in Fig. 1) to ensure that the pressure in the chamber was equal to ambient pressure and that there was no backflow from the main chamber to the pre-chamber: main chamber inlet (3), pre-chamber outlet (2), pre-chamber inlet (1), main chamber outlet (4). This ensures an overall uncertainty of 2 % in λ.

2.2 Schlieren measurements

The basic characterization of the ignition process inside the main chamber was done with a high-speed schlieren system (50 000 frames per second). The setup consisted of an LED ($\lambda = 635\,\mathrm{nm}$, $P = 205\,\mathrm{mW}$, 10° viewing angle), directly followed by a pinhole ($d = 0.2\,\mathrm{mm}$), whose light was collimated by a lens ($f = 500\,\mathrm{mm}$) and after passing the chamber focussed by another lens ($f = 1000\,\mathrm{mm}$). A second pinhole ($d = 1\,\mathrm{mm}$) was used for blocking refracted light. The schlieren images visualized the ignition and the subsequent flame propagation.

2.3 Pressure measurements

Two piezo-electric pressure sensors were used to observe the pressure evolution in the main chamber (Kistler Type 601 with Kistler amplifier Type 5015) and pre-chamber (Kistler 6113 – spark plug with integrated pressure sensor – with Kistler amplifier Type 5015). The results from the pressure curves achieved by turbulent hot jet ignition were related to spark plug ignition experiments, which were done in the same chamber, but without the pre-chamber, for best comparability. Here, only the main-chamber gas supply and the oxygen analyser for mixture control were used. To ensure atmospheric pressure in the

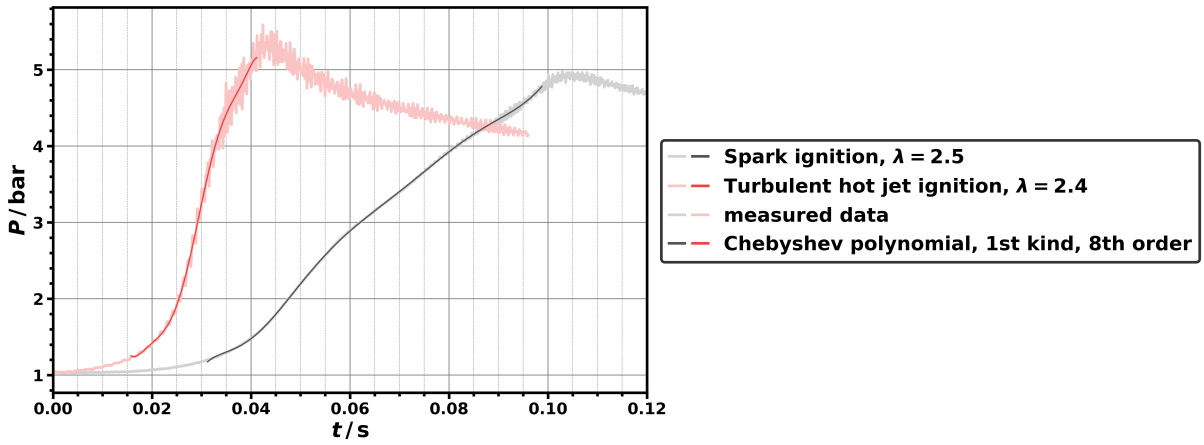

Figure 2: Comparison of two different pressure curves, one with spark ignition, one with turbulent hot jet ignition at similar air-fuel equivalence ratio (λ). When fitting the Chebyshev polynomial [11] for the determination of the maximum pressure rise, a larger time range is used than is actually evaluated in order to be able to eliminate any edge effects that may occur.

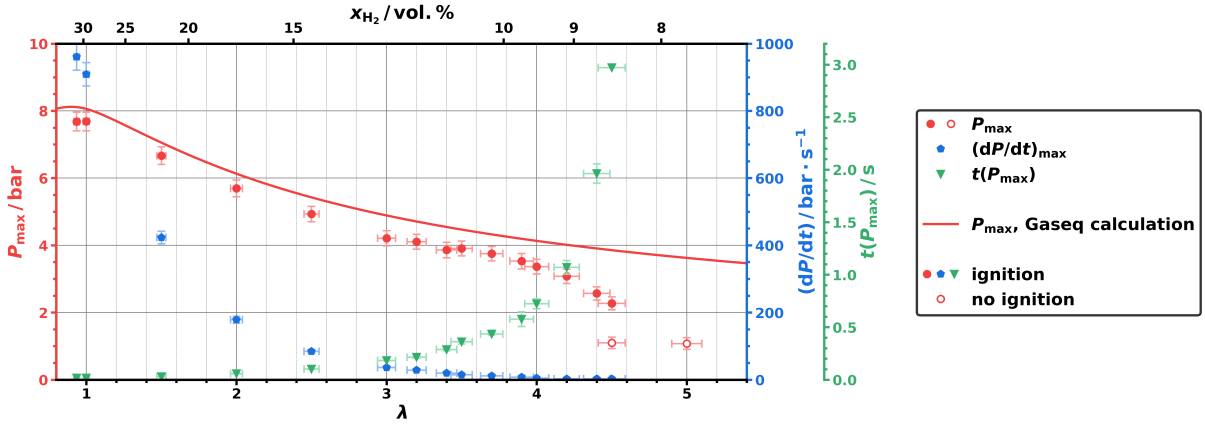

Figure 3: Reference measurements. Maximum pressure P_{max}, maximum pressure rise $(\mathrm{d}P/\mathrm{d}t)_{\mathrm{max}}$ and time of maximum pressure $t(P_{\mathrm{max}})$ in dependence of air-fuel equivalence ratio (λ) measured by spark ignition experiments in the test chamber. P_{max} additionally calculated with Gaseq [12].

vessel, valve 3 was closed before valve 4, when the oxygen concentration was stable. All pressure curves were analysed with respect to the maximum pressure P_{max}, the maximum pressure rise $(\mathrm{d}P/\mathrm{d}t)_{\mathrm{max}}$ and the delay time of maximum pressure to the spark ignition in the pre-chamber $t(P_{\mathrm{max}})$. They were corrected following the ideal gas law to similar conditions (25 °C and 1.00 bar) to account for variations in the initial conditions [10]. $(\mathrm{d}P/\mathrm{d}t)_{\mathrm{max}}$ was calculated via curve fitting (Chebyschev polynomial, 1$^{\mathrm{st}}$ kind, of 8$^{\mathrm{th}}$ order [11] fitted to the data between 5% and 95% of maximum overpressure; Fig. 2) and subsequent differentiation with determination of the maximum.

3 Results and Discussion

Lean mixtures with $\lambda > 3$ are of particular interest in this work due to their NO_x reduction potential. Hence, experiments were carried out mainly at the highest λ that still led to ignition. The lean ignition limit and combustion characteristics are explored for spark ignition and the THJI.

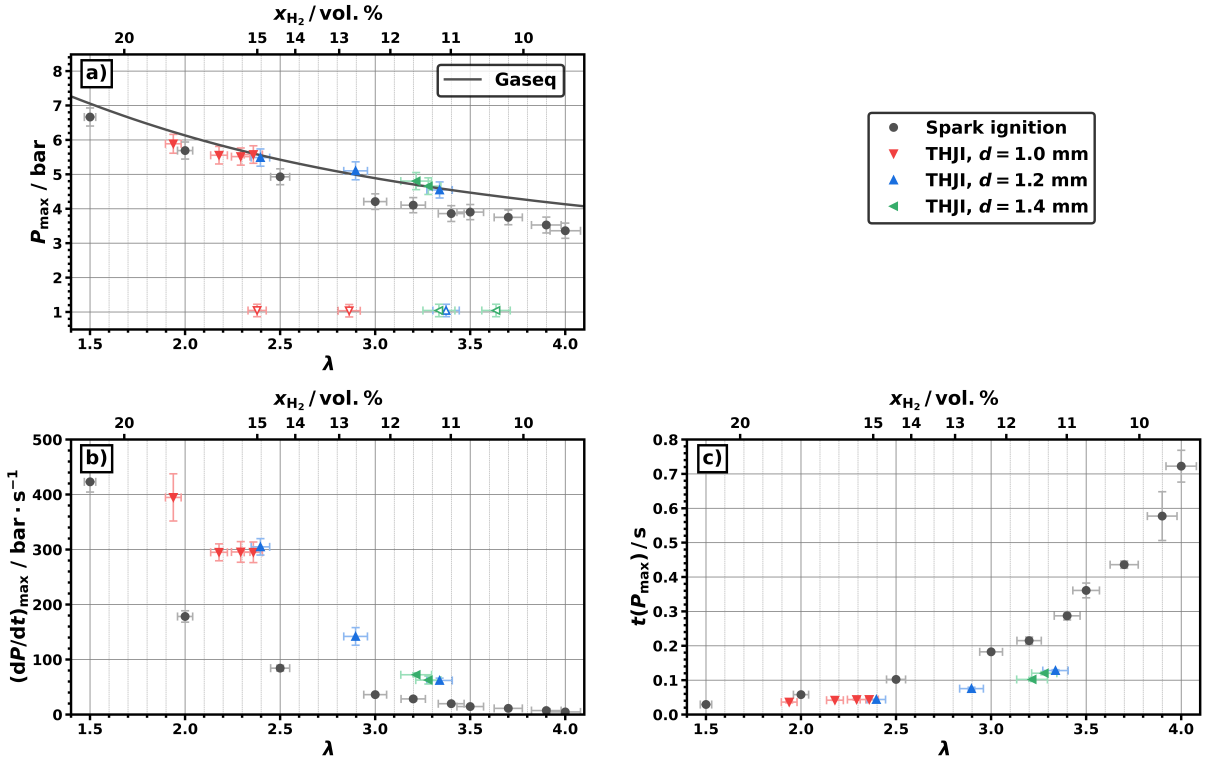

Figure 4: Comparison of maximum pressure P_{max}, maximum pressure rise $(\mathrm{d}P/\mathrm{d}t)_{\mathrm{max}}$ and time of maximum pressure $t(P_{\mathrm{max}})$ between spark plug ignition and turbulent hot jet ignition experiments with different orifice diameters d in dependence of air-fuel equivalence ratio (λ).

Fig. 2 shows two different pressure curves, once with spark ignition and once with turbulent hot jet ignition, at similar λ. It can be seen that with THJI the maximum pressure is reached earlier and is higher overall. A two-stage pressure rise can be observed in the spark ignition experiments, due to a change in flame shape [13]. The visible signal noise is an acoustical oscillation effect and not result of an error in the measurement setup. Due to this, $(\mathrm{d}P/\mathrm{d}t)_{\mathrm{max}}$ was calculated via curve fitting.

The reference pressure measurements from spark experiments (Fig. 3) show a strong decrease in $(\mathrm{d}P/\mathrm{d}t)_{\mathrm{max}}$ and P_{max} and a strong increase in $t(P_{\mathrm{max}})$ with increasing λ. The calculated P_{max} was always a bit higher than the measured one. Near the observed lean ignitability limit of $\lambda = 4.5$ the delay increases significantly. These effects are results of the slower laminar burning velocity [14].

The comparison between the spark ignition and THJI experiments is shown in Fig. 4. Independent of the orifice diameter, the measured P_{max} were higher, compared to spark ignition experiments, and closer to the Gaseq calculation. It was possible to ignite mixtures with $\lambda > 3$ by using orifice diameters of $d = 1.2\,\mathrm{mm}$ and $d = 1.4\,\mathrm{mm}$. With an orifice diameter of $d = 1.0\,\mathrm{mm}$ an ignitability limit of $\lambda = 2.4$ was observed. The obtained results are in a similar range to the results of [9]. However, a substantial improvement in burning characteristics was observed. The effect is most prominent in $(\mathrm{d}P/\mathrm{d}t)_{\mathrm{max}}$. At the same λ, $(\mathrm{d}P/\mathrm{d}t)_{\mathrm{max}}$ was almost twice as high as in spark ignition experiments. It appears that while the ignitability is a function of the orifice diameter, the pressure evolution is solely governed by the λ. As a result of the faster pressure evolution, $t(P_{\mathrm{max}})$ was significantly smaller, especially at higher λ. In terms of burn rate, the THJI with $\lambda = 3.3$ is comparable to the spark ignition with $\lambda = 2.5$.

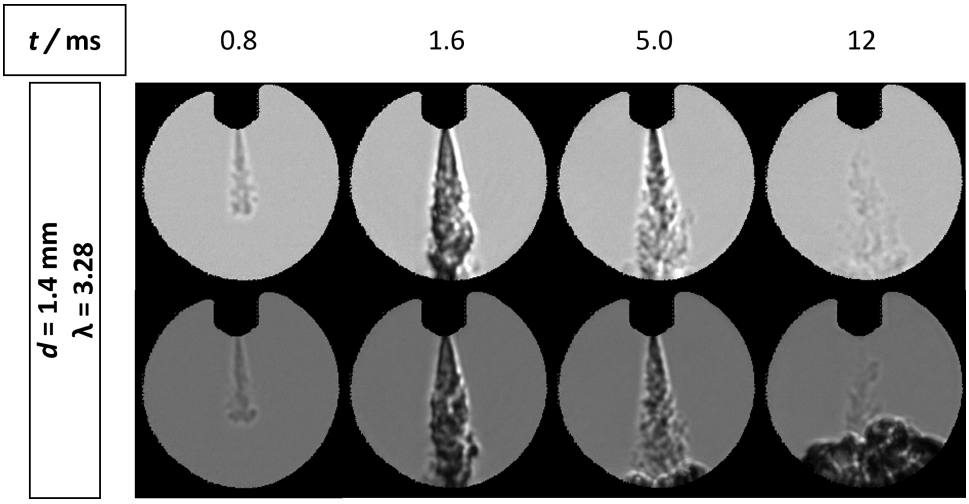

Figure 5: Exemplary schlieren images at different times after spark ignition inside the pre-chamber for a nozzle diameter of $d = 1.4\,\mathrm{mm}$ at the respective ignition limit, once with and once without ignition.

Exemplary schlieren images are shown in Fig. 5. Cold gas jets (0.8 ms) could be visualised as well as hot gas jets (1.6 ms) and the ignition inside the main chamber. At increased λ, the ignition occurs further downstream. The orifice has no effect on the location of the ignition. Instead, the ignition location seems to be influenced only by the λ. Qualitatively, additional schlieren images (not shown here) indicate a higher degree of turbulence in the free jet as the orifice diameter increases. Further, the images show the same penetration depth of the free jets regardless of the orifice diameter. Also, the pressure traces in the pre-chamber (pressure rise and maximum pressure) are almost identical for all orifice diameters. This indicates that the mass flux and, hence, the thermal energy transported in the jet, scales with d^2 in this experiment. Thus, ignition seems less likely for smaller orifices. However, turbulent mixing and complex heat transfer processes need to be accounted for, too. Hence, further experiments will be necessary to fully understand the different ignition behaviour of the orifice diameters.

Overall, the orifice diameter had an influence on the lean ignitability limit, but not on the subsequent combustion in the main chamber. For either orifice, once an ignition has been achieved, the combustion characteristics are significantly improved over the spark ignition base case. Particularly, the rate of pressure rise is about twice that of the spark ignition case.

4 Conclusions

The turbulent hot jet ignition of lean and ultra-lean hydrogen/air mixtures was studied experimentally. It was possible to ignite hydrogen/air mixtures with $\lambda > 3$ using THJI, but not with all orifice diameters investigated. Compared to spark ignition experiments, strongly improved combustion characteristics were observed, which make THJI to an interesting concept for reducing NO_x emission.

In the future, the influence of the pre-chamber λ on the THJI as well as pre-chambers with multiple orifices will be investigated. In addition, high-speed OH-LIF experiments will be integrated into the setup.

Acknowledgement

This work was funded by the Ministry of Science and Culture in Lower Saxony (MWK) in the Innovation Laboratory WaVe "Nachhaltige Wasserstoff-Verbrennungs-Konzepte".

References

[1] A. M. Oliveria, R. R. Beswick, and Y. Yan, "A green hydrogen economy for a renewable energy society," *Current Opinion in Chemical Engineering*, vol. 33, p. 100701, 2021.

[2] L. M. Das, "Exhaust emission characterization of hydrogen-operated engine system: nature of pollutants and their control techniques," *International Journal of Hydrogen Energy*, vol. 16, pp. 765–775, 1991.

[3] M. Klell, H. Eichlseder, and A. Trattner, *Wasserstoff in der Fahrzeugtechnik: Erzeugung, Speicherung, Anwendung*, 4th ed. Wiesbaden: Springer Vieweg, 2018.

[4] C. White, R. Steeper, and A. Lutz, "The hydrogen-fueled internal combustion engine: a technical review," *International Journal of Hydrogen Energy*, vol. 31, pp. 1292–1305, 2006.

[5] S. Biswas and L. Qiao, "Ignition of ultra-lean premixed H_2/air using multiple hot turbulent jets generated by pre-chamber combustion," *Applied Thermal Engineering*, vol. 132, pp. 102–114, 2018.

[6] L. A. Lovachev, V. S. Babkin, A. V. V'Yun, V. N. Krivulin, and A. N. Baratov, "Flammability limits: An invited review," *Combustion and Flame*, vol. 20, pp. 259–289, 1973.

[7] E. Toulson and H. J. Schock, "A review of pre-chamber initiated jet ignition combustion systems," *SAE International Powertrain Fuels & Lubricants Meeting*, 2010.

[8] J. Hua, L. Zhou, Q. Gao, Z. Feng, and H. Wei, "Influence of pre-chamber structure and injection parameters on engine performance and combustion characteristics in a turbulent jet ignition (tji) engine," *Fuel*, vol. 283, p. 119236, 2021.

[9] S. Biswas and L. Qiao, "Prechamber hot jet ignition of ultra-lean H_2/air mixtures: Effect of supersonic jets and combustion instability," *SAE International Journal of Engines*, vol. 9(3), pp. 1584–1592, 2016.

[10] T. Krause, M. Meier, and J. Brunzendorf, "Influence of thermal shock of piezoelectric pressure sensors on the measurement of explosions pressures," *Journal of Loss Prevention on The Process Industries*, vol. 71, p. 104523, 2021.

[11] T. J. Rivlin, *Chebyshev Polynomials – From Approximation Theory to Algebra & Number Theory*, 2nd ed. New York: Wiley, 1990.

[12] C. Morley, "Gaseq – a chemical equilibrium program for windows," http://www.gaseq.co.uk/, version 0.79, Jan 2005.

[13] D. Dunn-Rankin and R. F. Sawyer, "Tulip flames: changes in shape of premixed flames propagation in closed tubes," *Experiments in Fluids*, vol. 24, pp. 130–140, 1998.

[14] J. Warnatz, "The structure of laminar alkane-, alkene-, and acetylene flames," *18th Symposium (International) on Combustion*, pp. 369–384, 1981.